Vesicular Glutamate Transporter 1 Knockdown in Infralimbic Prefrontal Cortex Augments Neuroendocrine Responses to Chronic Stress in Male Rats

Brent Myers,[1] Jessica M. McKlveen,[2] Rachel Morano,[2] Yvonne M. Ulrich-Lai,[2] Matia B. Solomon,[2] Steven P. Wilson,[3] and James P. Herman[2]

[1]Biomedical Sciences, Colorado State University, Fort Collins, Colorado 80523; [2]Psychiatry and Behavioral Neuroscience, University of Cincinnati, Cincinnati, Ohio 45237; and [3]Pharmacology, Physiology, and Neuroscience, University of South Carolina, Columbia, South Carolina 29208

Chronic stress-associated pathologies frequently associate with alterations in the structure and activity of the medial prefrontal cortex (mPFC). However, the influence of infralimbic cortex (IL) projection neurons on hypothalamic-pituitary-adrenal (HPA) axis activity is unknown, as is the involvement of these cells in chronic stress-induced endocrine alterations. In the current study, a lentiviral-packaged vector coding for a small interfering RNA (siRNA) targeting vesicular glutamate transporter (vGluT) 1 messenger RNA (mRNA) was microinjected into the IL of male rats. vGluT1 is responsible for presynaptic vesicular glutamate packaging in cortical neurons, and knockdown reduces the amount of glutamate available for synaptic release. After injection, rats were either exposed to chronic variable stress (CVS) or remained in the home cage as unstressed controls. Fifteen days after the initiation of CVS, all animals were exposed to a novel acute stressor (30-minute restraint) with blood collection for the analysis of adrenocorticotropic hormone (ACTH) and corticosterone. Additionally, brains were collected for *in situ* hybridization of corticotrophin-releasing hormone mRNA. In previously unstressed rats, vGluT1 siRNA significantly enhanced ACTH and corticosterone secretion. Compared with CVS animals receiving the green fluorescent protein control vector, the vGluT1 siRNA further increased basal and stress-induced corticosterone release. Further analysis revealed enhanced adrenal responsiveness in CVS rats treated with vGluT1 siRNA. Collectively, our results suggest that IL glutamate output inhibits HPA responses to acute stress and restrains corticosterone secretion during chronic stress, possibly at the level of the adrenal. Together, these findings pinpoint a neurochemical mechanism linking mPFC dysfunction with aberrant neuroendocrine responses to chronic stress. **(*Endocrinology* 158: 3579–3591, 2017)**

The neuroendocrine response to stress, defined as a real or perceived threat to homeostasis or well-being, is critical for mobilizing energy to facilitate organismal survival and adaptation (1). However, prolonged exposure to stress mediators increases susceptibility to numerous psychiatric and cardiometabolic disorders (2). Accordingly, stress responses need to be finely tuned and context appropriate (3). The hypothalamic-pituitary-adrenal (HPA) axis mediates the primary endocrine stress response and is initiated by corticotrophin-releasing hormone (CRH)–producing neurons in the paraventricular hypothalamus (PVN) (4). These cells stimulate adrenocorticotropic hormone (ACTH) secretion from the anterior pituitary, which then leads to the synthesis and release of

ISSN Print 0013-7227 ISSN Online 1945-7170
Printed in USA

Received 1 May 2017. Accepted 18 July 2017.
First Published Online 25 July 2017

Abbreviations: ACTH, adrenocorticotropic hormone; ANOVA, analysis of variance; AUC, area under the curve; CRH, corticotrophin-releasing hormone; CVS, chronic variable stress; GFAP, glial fibrillary acidic protein; GFP, green fluorescent protein; HPA, hypothalamic-pituitary-adrenal; Iba-1, ionized calcium-binding adapter molecule 1; IgG, immunoglobulin G; IL, infralimbic cortex; KPBS, potassium phosphate-buffered saline; mPFC, medial prefrontal cortex; mRNA, messenger RNA; NeuN, neuronal nuclear antigen; PH, posterior hypothalamus; PL, prelimbic cortex; PVN, paraventricular hypothalamus; RIA, radioimmunoassay; siRNA, small interfering RNA; SSC, saline sodium citrate; vGluT, vesicular glutamate transporter.

corticosterone from the adrenal cortex (5). Corticosterone signals throughout the body to regulate the numerous neural, behavioral, and metabolic aspects of homeostasis (6). Accordingly, regulation of CRH neurons requires the integration of multiple systems and engages key forebrain limbic circuits, including the hippocampus, amygdala, and medial prefrontal cortex (mPFC) (7, 8).

The mPFC is a vital region for many stress-related processes, including contextual appraisal and coping behavior (9–11). The infralimbic cortex (IL) component of the mPFC is prominently implicated in depression-related behavior in rodents (12, 13). Importantly, the IL shares homology with Brodmann area 25 (14), a focal point for human depressive pathology (15). Although dorsal aspects of mPFC, including prelimbic cortex (PL), have consistently been found to inhibit the HPA axis (16–20), relatively few studies have specifically targeted the IL, and results have been equivocal. Excitotoxic lesions of the IL prevent acute stress-induced CRH messenger RNA (mRNA) expression (17), suggesting the area may provide HPA axis excitation. In contrast, knockdown of the glucocorticoid receptor in the IL enhances corticosterone responses, pointing to a role in glucocorticoid negative feedback (12). Furthermore, recent studies indicate that chronic stress increases inhibition of IL principal output neurons (21), suggesting that inhibition of IL glutamatergic projections may be a component of the sequelae of chronic stress. In the current study, we examined the role of glutamate release from IL neurons in endocrine responses to acute and chronic stress.

To reduce output from IL neurons throughout the course of chronic variable stress (CVS), we targeted the expression of vesicular glutamate transporter (vGluT) 1. Vesicular transporters (vGluT1, vGluT2, and vGluT3) are necessary and sufficient for packaging glutamate into presynaptic vesicles and, consequently, glutamate-mediated excitation of postsynaptic targets (22–24). These transporters exhibit region-specific expression, with vGluT1 predominantly localized to cortical areas (25). Overexpression of vGluT1 increases glutamate packaging and excitatory postsynaptic currents, while mice heterozygous for a null allele show a reduction in both parameters (24). Furthermore, vGluT1 knockout mice exhibit docking and fusion of empty synaptic vesicles with no excitatory postsynaptic currents (23, 24).

In the current study, we used a lentiviral-packaged small interfering RNA (siRNA) targeting vGluT1 mRNA. The virus was injected into the IL of rats to selectively reduce the glutamatergic output of IL projection neurons without damaging local cellular networks. After confirming the efficacy of the construct to reduce vGluT1 mRNA and protein expression *in vivo*, we examined the consequences of chronically reduced IL output on the dynamics of HPA axis responses to acute psychogenic stress and CVS. Collectively, our findings identify a critical neurochemical mechanism linking hypofunction of the mPFC with endocrine dysregulation following prolonged stress.

Methods

Animals

Male Sprague-Dawley rats from Harlan (Indianapolis, IN) weighing 250 to 275 g upon arrival were single housed throughout the experiment in a temperature/humidity-controlled room on a 12:12 light:dark cycle (lights on 06:00, off at 18:00 hours). Food and water were available *ad libitum*, and rats were acclimated to the animal facility for 1 week before initiation of experiments. All experimental procedures were conducted in accordance with the National Institutes of Health Guidelines for the Care and Use of Animals and approved by the University of Cincinnati Institutional Animal Care and Use Committee and University of Cincinnati Institutional Biosafety Committee.

Lentiviral construct

A lentivirus transfer vector, based on a third-generation, self-inactivating transfer vector (26), was constructed. Viruses were generated by transfection of the transfer vector with three packaging plasmids (Addgene, Cambridge, MA), including psPAX2, pRSV-Rev, and pMD2.G, into 293T cells. Viruses were concentrated by high-speed centrifugation, purified by further centrifugation through 20% sucrose/Dulbecco's phosphate-buffered saline, and stored in 10% sucrose/Dulbecco's phosphate-buffered saline at −80°. Virus particle concentrations were determined by quantitative real-time polymerase chain reaction for proviral DNA 24 hours following transduction of 293T cells and are expressed as transducing units per microliter (tu/μL). A 363-bp piece of DNA from the rat vGluT1 complementary DNA was synthesized that included 151 bp of the 3' coding region and 212 bp of the 3' untranslated region. This corresponds to nucleotides 1656 to 2018 of GenBank accession no. NM_053859. This is a region of low homology with vGluT2 and vGluT3 and avoids all the putative transmembrane domains of the transporter. The fragment was cloned in antisense orientation into a lentivirus transfer vector that expressed an enhanced green fluorescent protein (GFP) reporter. This vector uses the phosphoglycerate kinase-1 promoter, which expresses well in rat brain and is primarily neuronal (27–29). A control virus was constructed similarly, using a transfer vector with the phosphoglycerate kinase-1 promoter driving expression of enhanced GFP alone.

Stereotaxic surgery

Animals were anesthetized (90 mg/kg ketamine and 10 mg/kg xylazine, intraperitoneally) followed by analgesic (butorphanol) and antibiotic (gentamicin) administration. Rats received bilateral 1 μL microinjections (5×10^6 tu/μL titer) into the IL (2.9 mm anterior to bregma, 0.6 mm lateral to midline, and 4.2 mm ventral from dura), as described previously (12, 30), of either the vGluT1 siRNA virus, GFP control, or media control [high-glucose Dulbecco's modified eagle media (Mediatech, Manassas, VA)] as an additional control in preliminary studies. All injections were carried out with a 25-gauge, 2-μL microsyringe (Hamilton,

Reno, NV) using a microinjection unit (Kopf, Tujunga, CA) at a rate of 5 min/μL. To reduce tissue damage and allow diffusion, the needle was left in place for 5 minutes before and after injections. Animals recovered for 6 weeks before commencing experiments, corresponding to timeframes previously used for similar lentiviral systems (27–29).

In situ hybridization

Preparation of complementary RNA probes to vGluT1 was carried out as previously described (25, 31, 32). Coronal cryostat sections (15 μm thick) were cut through mPFC, mounted onto Superfrost Plus (Fisher Scientific, Pittsburgh, PA) slides, and stored at –20°C. For hybridization, slides were washed in diethyl pyrocarbonate–treated potassium phosphate-buffered saline (KPBS), acetylated, delipidated in chloroform, and dehydrated through a graded ethanol series. Each riboprobe was diluted (1.0×10^6 cpm/50 μL) in hybridization buffer as described previously (33). Coverslipped slides were placed in hybridization chambers over blotting paper soaked in 50% formamide and incubated overnight at 55°C. Coverslips were then removed, and slides were washed in 0.2× saline sodium citrate (SSC). Slides were subsequently incubated in RNase A (100 μg/mL) for 30 minutes at 37°C, washed three times (5 minutes each) in 0.2× SSC, incubated in 0.2× SSC for 1 hour at 65°C, and dehydrated through a graded ethanol series. Slides were then exposed on Kodak Biomax MR-2 Film (Eastman Kodak, Rochester, NY) and stored in a light-free environment for 14 days.

Riboprobes complementary to CRH mRNA were generated as previously described (33–35). Paraformaldehyde-fixed brains were sectioned (30 μm thick) through the hypothalamus on a freezing microtome (Leica, Buffalo Grove, IL) and stored at –20°C in cryoprotectant solution. For hybridization, sections were rinsed twice (5 minutes each) with 50 mM diethyl pyrocarbonate–treated KPBS, twice in KPBS containing 0.2% glycine, and twice again in KPBS. The sections were then treated with 0.25% acetic anhydride (in 0.1 M triethanolamine, pH 8.0) for 10 minutes and rinsed twice in 2× SSC before being dehydrated in a graded ethanol series. The transcription reactions were carried out as previously described for floating sections (36, 37). Briefly, the transcription reaction was incubated at 37°C for 60 minutes, and the labeled probe was separated from free nucleotide by ammonium acetate precipitation. Sections were then hybridized overnight with ^{35}S-labeled probe at 45°C in humidified incubation chambers. The next morning, sections were rinsed in 2× SSC, treated with RNAse A (100 μg/mL for 1 hour at 37°C), washed in decreasing concentrations of SSC (2× to 0.5× at room temperature), and incubated in 0.5× SSC (1 hour at 45°C) as previously described (36, 37). Sections were mounted onto Superfrost Plus slides, dehydrated through graded ethanol, air dried, and exposed to Kodak Biomax MR-2 film in a light-free environment for 7 days.

Image analysis for *in situ* hybridization

Autoradiographic film images of hybridized brain sections were captured by a digital camera with four sections sampled/animal and averaged to provide a single mean. Semiquantitative analyses of autoradiograph images were performed using Scion Image software, and hybridization signal was expressed as corrected gray level. The gray-level signal of the region of interest was corrected by subtracting the background gray-level signal. Standards were also measured using Scion Image to verify that all quantified gray levels were on the linear range of the film.

Immunohistochemistry

For single immunolabeling of GFP, tissue sections were washed in 50 mM KPBS and incubated in blocking buffer (50 mM KPBS, 0.1% bovine serum albumin, and 0.2% TritonX-100) for 1 hour at room temperature. Sections were placed in rabbit anti-GFP primary antibody (1:1000 in blocking buffer; Invitrogen, La Jolla, CA) overnight at 4°C. Following incubation, sections were rinsed and placed into Alexa488-conjugated donkey anti-rabbit immunoglobulin G (IgG; 1:500 in blocking buffer; Jackson Immunoresearch, West Grove, PA) for 30 minutes. Sections were rinsed, mounted onto slides, and cover slipped. Dual fluorescent immunolabeling was performed as described previously, with GFP labeled in sequence with either vGluT1, neuronal nuclear antigen (NeuN), astrocytic marker glial fibrillary acidic protein (GFAP), or microglial label ionized calcium-binding adapter molecule 1 (Iba-1). vGluT1 was visualized with rabbit anti-vGluT1 primary antibody (1:1000; Synaptic Systems, Goettingen, Germany) followed by Cy3-conjugated donkey anti-rabbit IgG (1:500; Jackson ImmunoResearch, West Grove, PA). To investigate lentiviral specificity, neural and glial markers were colabeled with GFP. NeuN was labeled with mouse anti-NeuN primary antibody (1:200; Millipore, Billerica, MA) and Cy5-conjugated goat anti-mouse IgG (1:500; Jackson ImmunoResearch). GFAP was visualized with rabbit anti-GFAP primary antibody (1:2000; Dako, Carpinteria, CA) and Cy3-conjugated donkey anti-rabbit IgG (1:500; Jackson ImmunoResearch). Iba-1 was labeled with rabbit anti-Iba-1 primary antibody (1:75; Abcam, Cambridge, MA) and Cy3-conjugated donkey anti-rabbit IgG (1:500; Jackson ImmunoResearch).

Imaging and analysis

For quantification of GFP and vGluT1 colocalization, digital images were captured from a 1-in-12 series with a Zeiss AxioObserver microscope using optical sectioning (63× objective) to permit quantification of colocalization within a given z-plane (0.5-μm thickness). The length of GFP-positive projections, as well as the length of vGluT1-positive immunofluorescence on GFP-positive projections, were measured using Axiovision. Length measurements were collected from three individual z-planes from each image stack with three image stacks collected per animal and resulting values averaged. Colocalizations were defined as white fluorescence from overlap between labeled GFP terminals and magenta-colored vGluT1. All other analysis of potential colabeling with GFP (NeuN, GFAP, and Iba-1) was carried out on images collected with a 20× objective. For each figure, brightness and contrast were enhanced uniformly using Adobe Photoshop (CC 14.2).

Stress protocols and experimental design

After initial experiments confirming the efficacy and selectivity of the vGluT1 siRNA construct, a cohort of rats (N = 50) was injected with either the lentiviral-packaged vGluT1 siRNA (n = 25) or GFP (n = 25). This cohort was further divided into groups that underwent CVS for 14 days (n = 14 per microinjection group) or remained in the homecage as unstressed controls (n = 11 per microinjection group). However, all animals were handled regularly for body weight monitoring. The

CVS was comprised of twice daily (AM and PM) repeated and unpredictable stressors, including exposure to brightly-lit open field (1 m^2, 5 minutes), cold room exposure (4°C, 1 hour), forced swim (23° to 27°C, 10 minutes), brightly-lit elevated platform (0.5 m, 5 minutes), shaker stress (100 rpm, 1 hour), and hypoxia (8% oxygen, 30 minutes). Additionally, overnight stressors were variably included, comprised of social crowding (six to eight rats/cage, 16 hours) and restricted housing (mouse cage, 16 hours). On day 15, all rats were exposed to a novel acute restraint to directly compare the effects of vGluT1 knockdown on endocrine responses to acute and chronic stress.

Blood collection

The morning after completion of CVS (at least 16 hours after last stress exposure), all animals were exposed to a novel 30-minute restraint. Stress response assessment was initiated between 08:00and 09:00 hours, near the circadian trough of corticosterone secretion. Animals were placed in well-ventilated Plexiglas restraint tubes, and blood samples (approximately 250 μL) were collected by tail clip in tubes containing 10 μL of 100 mmol/L ethylenediamine tetraacetate. Samples were collected before (0 minutes) and 15, 30, 60, and 90 minutes after onset of 30-minute restraint stress and immediately placed on ice. Each sample was collected in less than 3 minutes, prior to rises in ACTH or corticosterone due to sampling (38). Blood samples were centrifuged at 3000× g for 15 minutes at 4°C, and plasma was stored at –20°C until radioimmunoassay (RIA).

Tissue collection

On day 16, 24 hours after acute restraint, all animals were given an overdose of sodium pentobarbital and transcardially perfused with 0.9% saline followed by 4% phosphate-buffered paraformaldehyde. Brains were postfixed in paraformaldehyde for 24 hours and then stored in 30% sucrose at 4°C. Brains were subsequently sectioned and processed for GFP immunohistochemistry (described previously) to determine microinjection spread and CRH *in situ* hybridization (described previously). Adrenal glands were also dissected and weighed as somatic indices of CVS exposure.

RIA

Plasma ACTH was determined by an RIA that uses a specific antiserum (1:120,000 dilution; donated by Dr. William Engeland from the University of Minnesota) with ^{125}I ACTH (Amersham Biosciences, Piscataway, NJ) as labeled tracer (39). All samples were run in duplicate in the same assay. Coefficient of variation for ACTH RIA was 7.6% intra-assay and 13.3% interassay. Plasma corticosterone levels were measured with an ^{125}I RIA kit (MP Biomedicals, Orangeburg, NY) (40). All samples were run in duplicate, and all time points were run in the same assay. For corticosterone RIA, intra-assay coefficient of variation was 8.6% and interassay 13.6%.

Data analysis

Data are expressed as mean ± standard error of the mean. All data were analyzed with GBStat (Dynamic Microsystems, Silver Spring, MD). vGluT1 mRNA and GFP/vGluT1 colocalization were analyzed with unpaired *t* tests. Body weight, plasma ACTH time courses, and plasma corticosterone time courses were analyzed by three-way repeated-measures analysis of variance (ANOVA), with treatment, stress, and time as factors. *Post hoc* tests were only conducted when significant main effects were reported, and differences at individual time points were assessed using Fisher least significant difference *post hoc* test. Adrenal index (g/g body weight), CRH mRNA, basal corticosterone, integrated hormonal exposure [area under the curve (AUC)], and adrenal responsivity were all analyzed by two-way ANOVA, with treatment and stress as factors. Main effects of treatment or stress were further assessed using Fisher's lease significant difference *post hoc* test. Adrenal responsivity was determined by dividing the integrated concentration of corticosterone by the log of the integrative concentration of ACTH (41). Corrected adrenal responsivity was calculated by dividing adrenal responsivity by the adrenal index. Statistical significance was set at $P < 0.05$ for all tests.

Results

Verification of vGluT1 knockdown

Injection of lentiviral-packaged constructs into the IL led to successful transduction as evidenced by GFP immunoreactivity [Fig. 1(a) and 1(d)]. Further, *in situ* hybridization (four hybridization images/animal) indicated that the vGluT1 siRNA (n = 7) significantly ($P < 0.05$) decreased vGluT1 mRNA in the IL compared with GFP controls (n = 5) [$t(10) = 2.74$, $P = 0.02$] [Fig. 1(b)]. Analysis of vGluT1 mRNA in the PL indicated that treatment effects were specific to the IL, as the siRNA (n = 7) did not significantly alter vGluT1 expression compared with GFP (n = 5) [$t(10) = 1.61$, $P = 0.14$] [Fig. 1(c)]. As the siRNA approach is a post-transcriptional intervention, we sought to quantify vGluT1 protein expression within IL projections. GFP-positive projections into the neighboring orbital cortex were imaged in the z-plane to quantify the percent length of GFP-positive projections that colocalize with vGluT1 protein. This length was measured in three individual z-slices (0.5-μm thickness) per image stack, with three stacks collected per animal for a total of nine quantified images/animal. The vGluT1 siRNA (n = 3) significantly ($P < 0.05$) decreased the percent length of GFP-positive projections that express vGluT1 protein [$t(4) = 3.65$, $P = 0.02$] compared with GFP controls (n = 3) [Fig. 1(e)].

Lentiviral selectivity

Efficacy and selectivity of the lentiviral-packaged vGluT1 siRNA was further examined through immunohistochemical analysis. Viral media was injected as an additional control [Fig. 2(a), 2(d), 2(g), and 2(j)] and compared with the GFP control vector [Fig. 2(b), 2(e), 2(h), and 2(k)]. Relative to media injection, the GFP control did not alter vGluT1 expression, neuronal viability (NeuN), astrocytic (GFAP) number or morphology, or microglial (Iba-1) number or morphology. Furthermore, neither the GFP nor the vGluT1 siRNA constructs were expressed in astrocytes or microglia. Whereas the vGluT1 siRNA did not diminish neuronal viability or

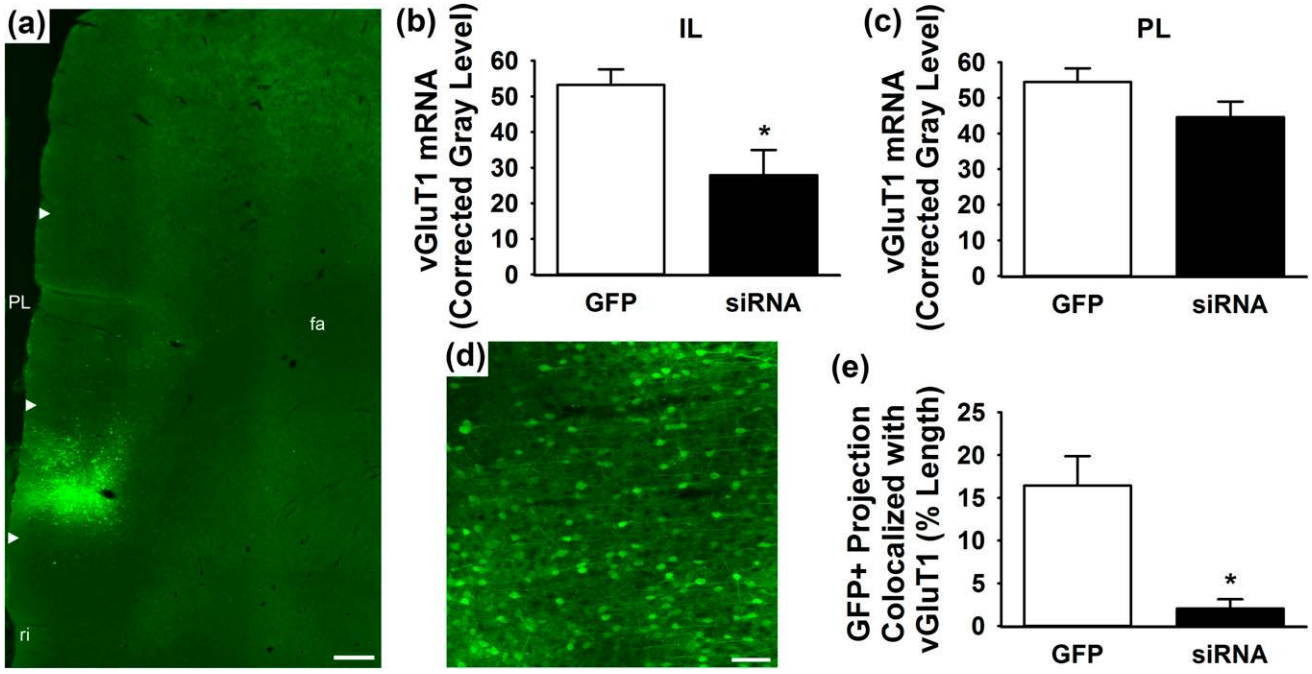

Figure 1. (a) Lentiviral injections targeted the IL with minimal spread to PL. White arrow heads indicate dorsal and ventral boundaries of IL and PL. (b) The vGluT1 siRNA (n = 7) decreased vGluT1 mRNA compared with GFP controls (n = 5). (c) Lentiviral treatment did not affect vGluT1 mRNA expression in the PL. (d) Lentiviral infection and gene transfer is evidenced by GFP immunoreactivity. (e) The vGluT1 siRNA (n = 3) decreased the percent length of GFP-positive projections expressing vGluT1 protein compared with GFP controls (n = 3). * $P < 0.05$ compared with GFP. Scale bar (a) = 300 μm, scale bar (d) = 100 μm. fa, anterior forceps of the corpus callosum; ri, rhinal incisure.

induce gliosis, the construct markedly reduced the expression of vGluT1 protein at GFP-positive terminals [Fig. 2(c), 2(f), 2(i), and 2(l)].

Microinjection placement

To examine spread of viral microinjections, single-label GFP immunohistochemistry was used to map the total spread of individual injections. The individual injection profiles were then overlaid onto a single atlas template (Fig. 3) adapted from Swanson (42). This composite illustrates that most injections spread throughout the mid and rostral IL, with limited spread into the neighboring PL. Injections with major spread into the PL (defined as more than 20%) were excluded, thus the viral treatments in the current study predominantly affected the IL. After determining injection placement and spread, three rats were removed from the study due to failed injections.

Somatic markers of chronic stress

Postmortem tissue analysis indicated a main effect of CVS [$F(1, 43) = 28.65$, $P < 0.0001$] to increase adrenal weight relative to body weight [Fig. 4(a)], with no effect of virus injection. *Post hoc* analysis confirmed that the CVS GFP (n = 14, $P < 0.001$) and CVS siRNA groups (n = 11, $P < 0.05$) exhibited adrenal hypertrophy relative to the no-CVS GFP and no-CVS siRNA groups (n = 11 per group), respectively. There was also a main effect of CVS to decrease body weight gain [$F(4, 172) = 11.88$, $P = 0.0013$]. Specifically, CVS GFP and CVS siRNA groups (n = 11 to 14 per group) had significantly lower body weight [Fig. 4(b)] compared with within-treatment, no-CVS controls (n = 11 per group) on days 9, 12, and 15 of stress exposure.

PVN CRH expression

On the morning of day 16 (24 hours after acute restraint), there was a main effect of treatment to increase CRH mRNA expression in the PVN (Fig. 5). The vGluT1 siRNA increased CRH expression compared with GFP [$F(1, 88) = 4.09$, $P = 0.046$] (n = 11 to 14 per group) with no significant within-treatment or within-stress differences.

ACTH and corticosterone responses to acute and chronic stress

Although hormonal time course data for all groups was analyzed by three-way repeated-measures ANOVA, the time profiles of no-CVS and CVS animals are shown separately for clarity of treatment effects. In terms of the ACTH response to restraint stress, there was a significant stress × treatment × time interaction [$F(4, 172) = 13.48$, $P < 0.0001$] [Fig. 6(a) and 6(c)]. Compared with no-CVS GFP rats, no-CVS siRNA animals had significantly ($P < 0.01$) higher plasma ACTH 15 and 30 minutes after the initiation of restraint stress (n = 11 per group). In animals with a history of CVS, the siRNA group (n = 11) exhibited significantly ($P < 0.01$) lower ACTH 15 minutes after the

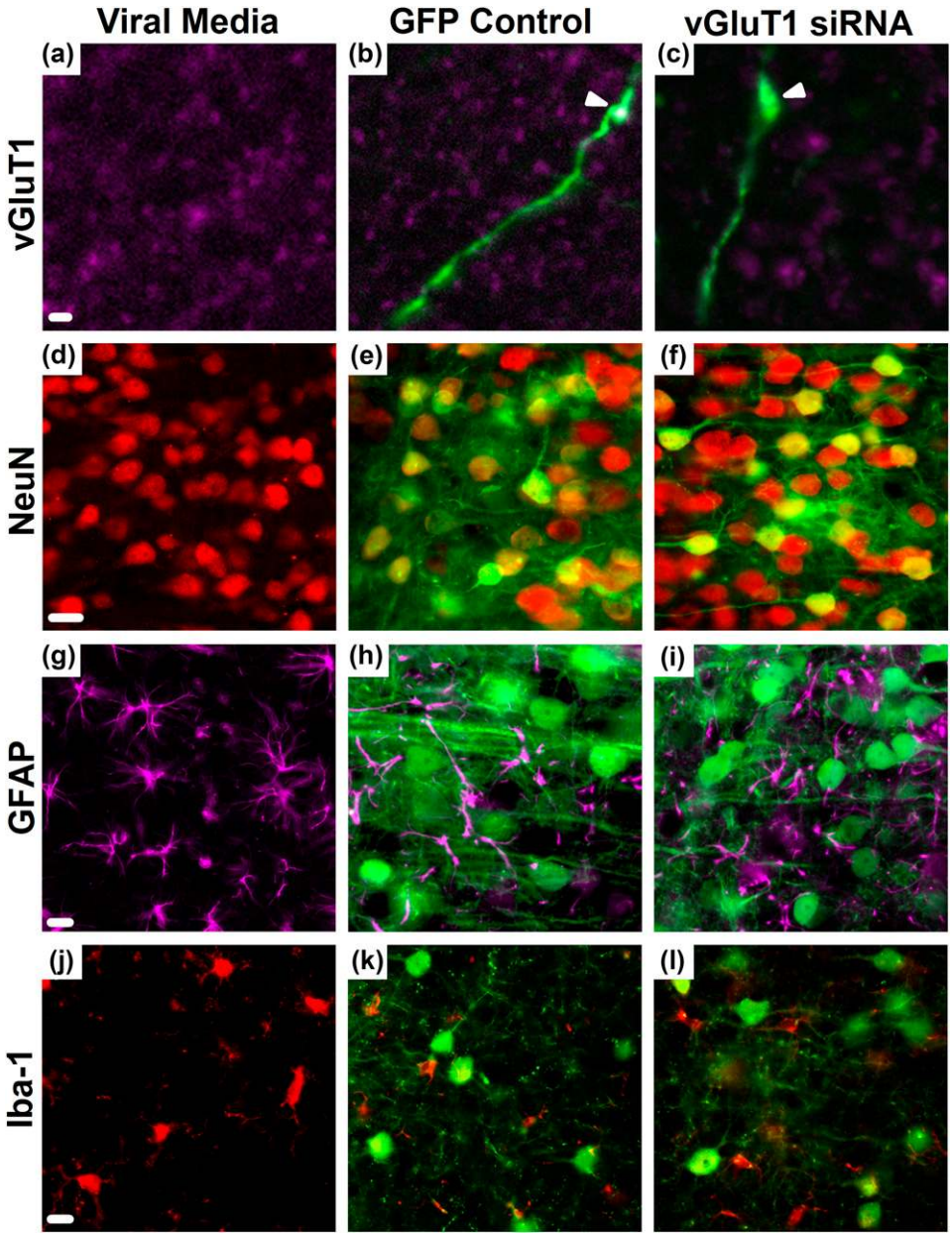

Figure 2. (a) Expression of vGluT1 protein (magenta) in the absence of viral gene transfer. Immunolabeling of GFP (green) and vGluT1 (magenta) proteins demonstrated (b, arrowhead) colabeling in GFP controls that was decreased by the (c, arrowhead) siRNA in GFP-expressing IL projections. (d–f) GFP colocalized with NeuN (red), indicating neuronal viability was maintained following infection. The astrocyte marker (g–i) GFAP (magenta) and (j–l) microglia/macrophage marker Iba-1 (red) did not indicate colocalization with GFP or frank gliosis. Media controls received viral media in the absence of gene transfer. Scale bars (a–c) = 5 μm, scale bars (d–l) = 20 μm.

initiation of restraint compared with GFP controls (n = 14).

Corticosterone responses to restraint were increased by vGluT1 knockdown, as there was a significant treatment × time interaction [$F(4, 172) = 5.15$, $P = 0.0006$] [Fig. 6(b) and 6(d)]. In animals without a prior history of stress, the siRNA significantly ($P < 0.01$) increased corticosterone 60 minutes after the stressor was presented (n = 11 per group). In GFP-treated rats, CVS significantly ($P < 0.05$) facilitated corticosterone secretion at 0 and 15 minutes (n = 11 to 14 per group). However, chronically stressed rats that received the vGluT1 siRNA (n = 11) had significantly increased plasma corticosterone 0 ($P < 0.001$), 30 ($P < 0.05$), and 60 ($P < 0.01$) minutes after the beginning of restraint compared with CVS GFP rats (n = 14).

Basal and integrative HPA profiles

Basal (0-minute) corticosterone values compared across all groups [Fig. 7(a)] demonstrate a significant treatment × stress interaction [$F(1, 46) = 7.47$, $P = 0.009$]. CVS GFP rats (n = 14) had significantly ($P < 0.05$) higher basal corticosterone than no-CVS GFP animals (n = 11). Further, CVS siRNA animals (n = 11) had significantly higher basal corticosterone than both the no-CVS siRNA

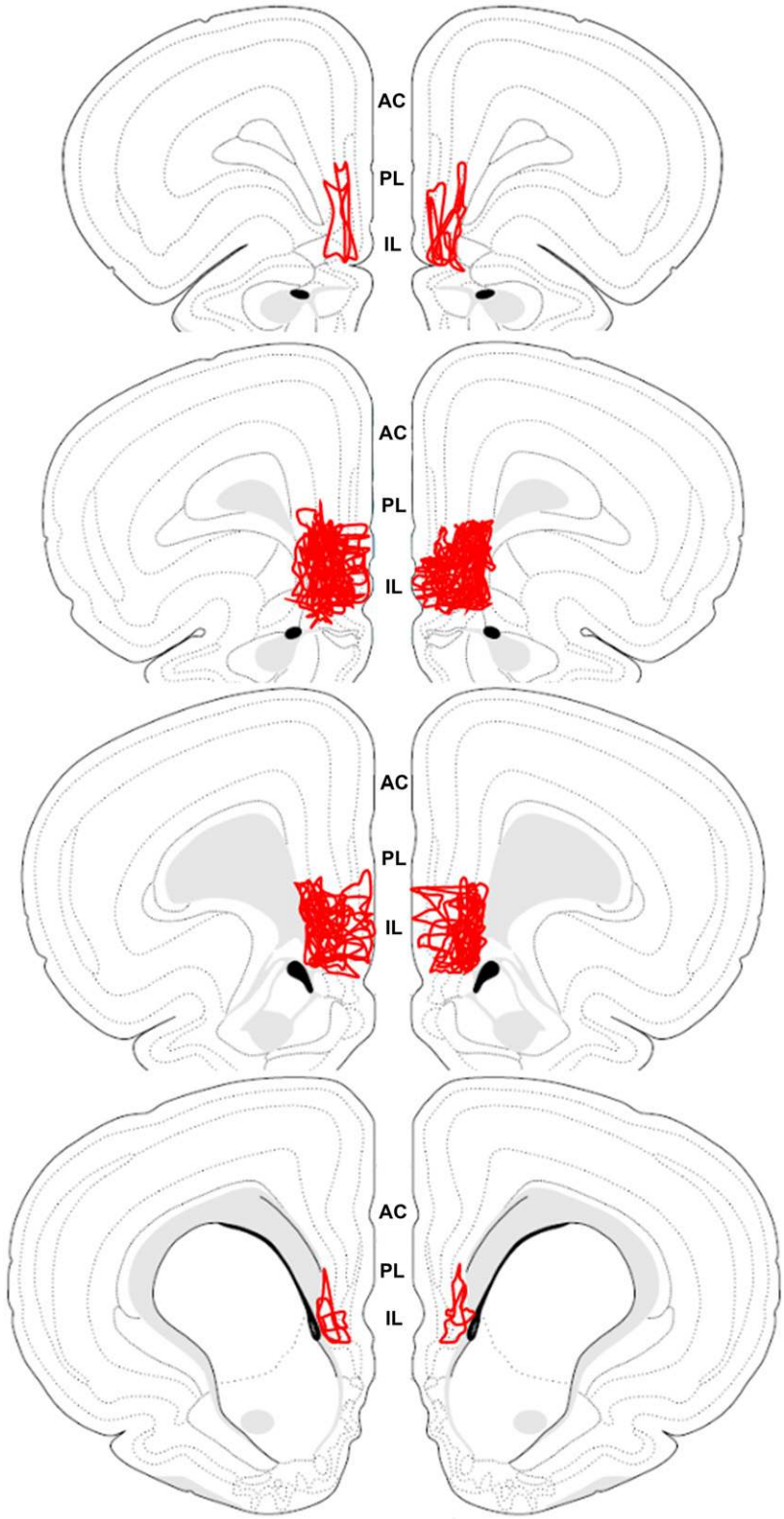

Figure 3. The spread of all individual injections was overlaid onto a single atlas template (42). The schematic illustrates that injections primarily spread throughout the IL with limited spread into the neighboring PL. AC, anterior cingulate.

($P < 0.001$) and CVS GFP groups ($P < 0.001$) (n = 11 to 14 per group), indicating that vGluT1 knockdown interacts with CVS to promote basal glucocorticoid hypersecretion.

Analysis of cumulative exposure to HPA hormones in the form of time-integrated AUC revealed additional interactions between vGluT1 knockdown and chronic stress [Fig. 7(b) and 7(c)]. There was stress × treatment interaction for the ACTH AUC [$F(1, 46) = 12.33$, $P < 0.001$]. In no-CVS animals, the siRNA increased cumulative ACTH exposure ($P < 0.01$). However, the CVS siRNA group had significantly ($P < 0.001$) less ACTH release compared with no-CVS siRNA rats, with no within-CVS differences.

The integrated corticosterone response exhibited main effects of stress [$F(1, 46) = 8.07$, $P = 0.007$] and treatment [$F(1, 46) = 18.85$, $P < 0.001$]. Specifically, the no-CVS siRNA group had higher ($P < 0.01$) cumulative corticosterone exposure than no-CVS GFP rats. The CVS siRNA rats had corticosterone responses greater than both CVS GFP ($P < 0.001$) and no-CVS siRNA ($P < 0.05$) groups.

Adrenal responsivity

Adrenal responsivity, calculated as the cumulative corticosterone concentration divided by the log of the cumulative ACTH concentration [Fig. 7(d)], is a standard, yet indirect, index of adrenal sensitivity to ACTH (19, 30, 41). There were main effects of stress [$F(1, 46) = 27.11$, $P < 0.001$] and treatment [$F(1, 46) = 17.72$, $P < 0.001$] on adrenal responsivity. Further analysis indicated that the CVS GFP group (n = 14) had higher ($P < 0.05$) adrenal responsivity compared with no-CVS GFP rats (n = 11). Additionally, the CVS siRNA rats had greater responsivity than both CVS GFP ($P < 0.001$) and no-CVS siRNA ($P < 0.001$) groups (n = 11 to 14 per group). Adrenal responsivity was corrected for adrenal index to examine the degree to which increased adrenal responsivity could be attributed to adrenal hypertrophy: [(corticosterone AUC/logACTH AUC)]/[(adrenal weight/body weight) × 100] [Fig. 7(e)]. There were main effects of stress [$F(1, 46) = 5.09$, $P = 0.029$] and treatment [$F(1, 46) = 13.71$, $P = 0.0006$] on

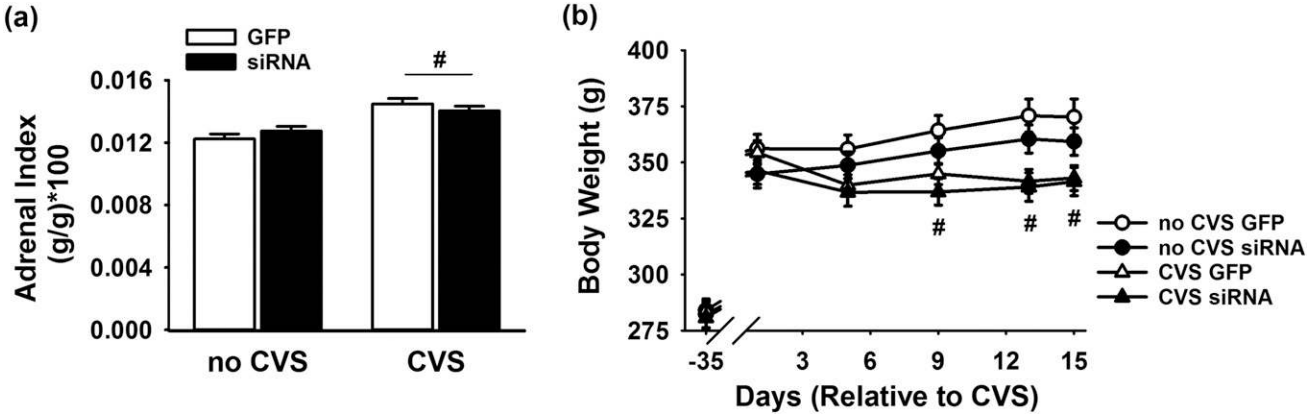

Figure 4. (a) There was a main effect of CVS to increase adrenal weight relative to body weight (n = 11 to 14 per group). (b) Both CVS GFP and CVS siRNA groups (n = 11 to 14 per group) had lower body weight compared with within-treatment, no-CVS controls (n = 11 per group) on days 9, 12, and 15 of stress exposure. $^{\#}P < 0.05$ compared with no CVS.

corrected adrenal responsivity. Additionally, the CVS siRNA group had higher corrected adrenal responsivity than the no-CVS siRNA ($P < 0.05$) and CVS GFP ($P < 0.001$) groups (n = 11 to 14 per group).

Discussion

In the current study, we developed an approach to selectively reduce the output of IL glutamatergic neurons. A lentiviral-packaged siRNA construct was used to selectively reduce the expression of vGluT1 at the terminals of IL projection neurons. Using this approach, we tested the importance of IL glutamatergic output for regulating HPA axis dynamics following acute and chronic stress. In rats exposed to a single acute stressor, the reduction in vGluT1 enhanced CRH expression, elevated ACTH release, and amplified peak corticosterone responses. Further, knockdown of vGluT1 substantially augmented endocrine responses to chronic stress. Animals that underwent CVS with reduced IL output displayed increased CRH expression, reduced ACTH, and elevated basal and stress-induced corticosterone secretion. Furthermore, adrenal responsivity was markedly enhanced in CVS rats with vGluT1 knockdown. Collectively, these results indicate that glutamatergic outflow from the IL is necessary to constrain activity throughout the HPA axis during an acute stressor and is required to limit the impact of chronic stress on basal HPA axis drive and sensitization of neuroendocrine responses at the level of the adrenal cortex.

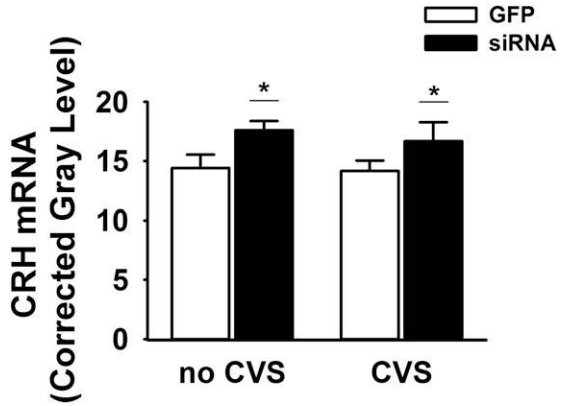

Figure 5. There was a main effect of siRNA treatment to increase CRH mRNA expression in the PVN 24 hours after acute restraint (n = 11 to 14 per group). $^{*}P < 0.05$ compared with GFP.

Previous examination of prefrontal regulation of HPA axis activity has produced divergent findings. Early studies from Diorio *et al.* (16) used lesions and local glucocorticoid implants to demonstrate that the mPFC inhibits ACTH and corticosterone stress responses. Interestingly, lesions of the mPFC facilitate responses to psychogenic but not systemic stressors (16, 20). Others have shown that large bilateral or right-sided mPFC lesions decrease corticosterone responses to repeated (but not acute) restraint, suggesting the mPFC may enhance corticosterone secretion in conjunction with exposure to a homotypic stress regimen (43). Pivotal work by Radley *et al.* (17) demonstrated that the mPFC regulates the HPA axis in a region-specific manner. Excitotoxic lesions of the PL increase CRH mRNA as well as ACTH and corticosterone stress responses. In contrast, IL lesions do not produce significant differences in HPA axis activation relative to sham-lesioned controls, but do markedly increase activation of PVN preautonomic neurons (17). Given the complexity of local interneuronal and glial networks in the mPFC, our approach of specifically reducing the outflow of the IL during stress exposure permits a highly selective examination of IL stress integration. Advancing previous studies that damaged the region, our results indicate that IL glutamate is critical for inhibiting basal and stress-induced HPA axis activity.

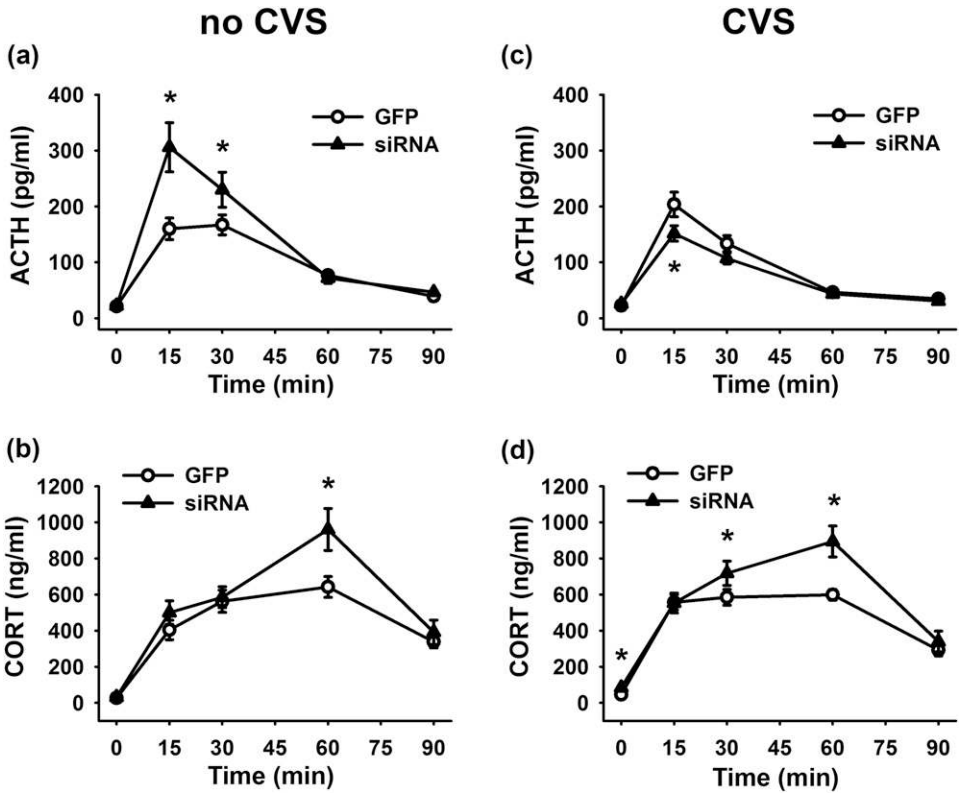

Figure 6. Hormonal time course data for all groups was collected and analyzed together, but acute stress (no CVS) and CVS animals are shown separately for clarity of treatment effects. (a) In previously unstressed rats, siRNA treatment increased plasma ACTH 15 and 30 minutes after the initiation of restraint stress (n = 11 per group). (b) The siRNA also increased corticosterone 60 minutes after the stressor was presented (n = 11 per group). (c) In animals with a history of CVS, the siRNA group (n = 11) exhibited lower ACTH 15 minutes after the initiation of restraint than GFP controls (n = 14). (d) In chronically stressed rats, the vGluT1 siRNA (n = 11) increased plasma corticosterone 0, 30, and 60 minutes after the beginning of restraint compared with CVS GFP rats (n = 14). $*P < 0.05$ compared with GFP. CORT, corticosterone.

Our group recently used a short hairpin RNA strategy to demonstrate that the glucocorticoid receptor in both the PL and IL mediates glucocorticoid negative feedback on corticosterone responses to acute stress (12). However, only the IL participates in feedback inhibition during CVS, suggesting the region may be particularly important for chronic stress adaptation. Combined with the finding that CVS increases presynaptic γ-aminobutyric acid (GABA) release onto IL glutamatergic neurons (21), these data suggest that the activity of principal glutamatergic projection neurons in the IL could be a critical regulator of endocrine homeostatic changes associated with chronic stress. Previous circuit mapping studies demonstrated that IL glutamatergic neurons innervate caudal regions of the hypothalamus implicated in stress responding (32). In particular, stress-activated IL projections target GABAergic neurons within the posterior hypothalamus (PH) (30). Furthermore, GABAergic signaling within the PH tonically inhibits excitatory output to PVN CRH neurons (30, 44). The results of the current study suggest that attenuating IL excitation of GABAergic cells within stress excitatory regions, such as the PH, may disinhibit neural and endocrine stress reactivity (Fig. 8). However, the approach used by the current study globally reduces IL output, and the observed effects could be mediated, in part, by multiple IL targets, including subnuclei of the amygdala (45).

The synaptic consequences of global vGluT1 deletion have been studied extensively in mice (22, 24). Not only does vGluT1 expression level dictate vesicular glutamate load and postsynaptic excitation, total loss of vGluT1 leads to the docking and fusion of empty vesicles (23). The long-term effects of vGluT1 reduction on synaptic homeostasis have been difficult to study as the knockout is developmentally lethal (22, 24). vGluT1 knockout mice typically survive up to 17 days and, at this age, show no changes in synaptic structure or in the expression of key synaptic proteins (24). However, in animals whose health can be maintained to 7 weeks, there is a reduction in the number of synaptic vesicles per terminal, although terminal number is unchanged (22). These animals also have reduced expression of proteins associated with neurotransmitter release, including synapsin 1, synaptobrevin, and rab3. Yet, even with global vGluT1 deletion for 7 weeks, there is no change in the size of the postsynaptic density (22). With

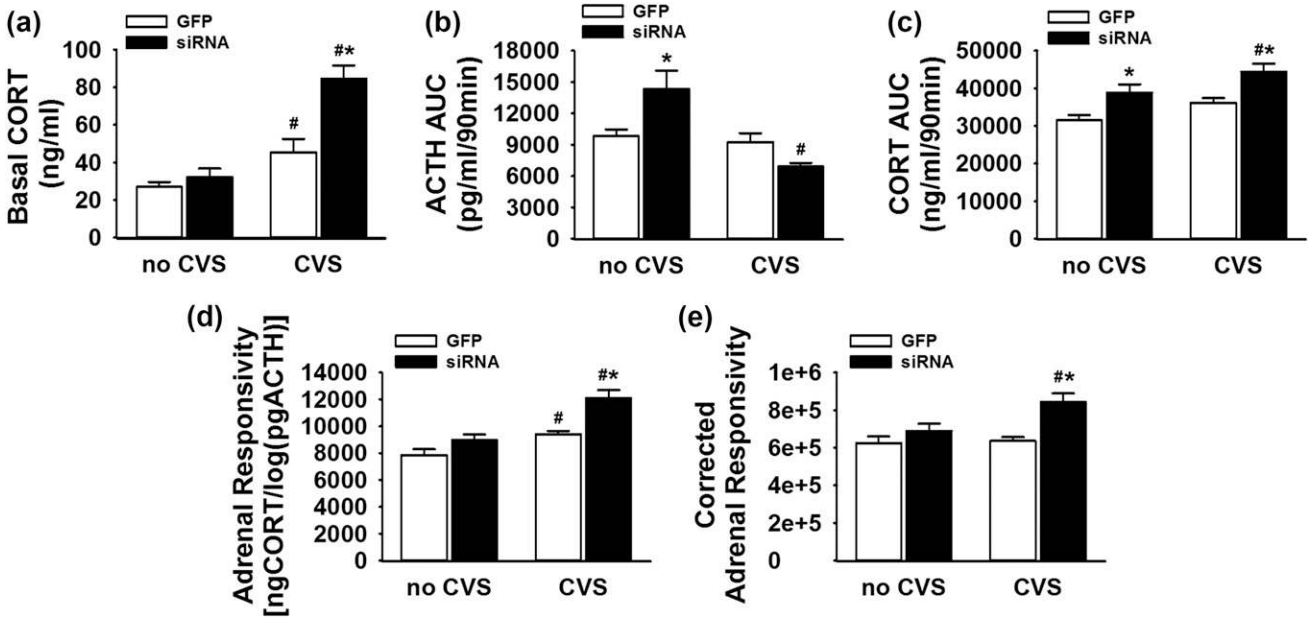

Figure 7. (a) CVS GFP rats (n = 14) had higher basal corticosterone than no-CVS GFP animals (n = 11). CVS siRNA animals had higher basal corticosterone than both the no-CVS siRNA and CVS GFP groups (n = 11 to 14 per group). (b) In no-CVS animals, the siRNA increased cumulative ACTH exposure, whereas the CVS siRNA group had less ACTH release compared with no-CVS siRNA rats (n = 11 to 14 per group). (c) The no-CVS siRNA group had higher cumulative corticosterone exposure compared with no-CVS GFP rats (n = 11 per group). The CVS siRNA rats had cumulative corticosterone responses greater than both CVS GFP and no-CVS siRNA groups (n = 11 to 14 per group). (d) The CVS GFP group had elevated cumulative adrenal responsivity compared with no-CVS GFP rats, whereas the CVS siRNA rats had greater responsivity than both CVS GFP and no-CVS siRNA groups (n = 11 to 14 per group). (e) Cumulative adrenal responsivity corrected for adrenal index indicated that CVS siRNA rats had enhanced adrenal responsivity compared with both CVS GFP and no-CVS siRNA groups: [ngCORT/log(pgACTH)]/[(adrenal weight/body weight) × 100] (n = 11 to 14 per group). $^{*}P < 0.05$ compared with within-stress GFP, $^{\#}P < 0.05$ compared with within-treatment, no-CVS controls. CORT, corticosterone.

respect to our viral-based approach, these findings suggest that postsynaptic compensation for reduced IL vGluT1 could be minimal, as long-term deletion only has minor effects on synaptic architecture.

One of the apparently paradoxical findings in the current study is that vGluT1 knockdown during CVS causes pronounced glucocorticoid hypersecretion in combination with diminished ACTH. Increased adrenal responsivity is not uncommon under certain conditions, including depression, aging, surgery, and illness (46–48). Increased adrenal responsivity is thought to be mediated by enhanced sympathetic neural and/or immune input to the adrenal gland that disassociates glucocorticoid production from ACTH levels (49), representing a mechanism whereby chronic stress (or illness) can maintain elevated steroidogenesis despite a normalization of circulating ACTH by glucocorticoid negative feedback (50). In this regard, it is important to note that IL damage increases activation of presympathetic neurons in the PVN (17). Consequently, it is possible that loss of IL glutamate release causes changes in sympathetic output that may be sufficient to enhance adrenal sensitivity to ACTH.

Limitations and future studies

Although analysis of responsivity suggests altered adrenal function plays an important role in IL-mediated responses to chronic stress, this is an indirect measure. Future studies of *in vivo* adrenal sensitivity to exogenous ACTH would provide more direct evidence. Additionally, adrenal responsivity interacts with adrenal weight, making *in vitro* studies of zona fasciculata cells necessary for direct evidence of increased cellular sensitivity to ACTH. Sustained elevations in ACTH associated with prolonged stress induce adrenocortical cellular hypertrophy leading to increased adrenal weight; furthermore, neural inputs are able to stimulate cellular proliferation in the case of compensatory adrenal growth (51–54). The potential interactions of these mechanisms with the augmented chronic stress reactivity outlined in the current study remain to be determined.

Rats in the current study were housed in the vivarium for approximately 8 weeks prior to the CVS component of the experiment; however, it is possible that responses to CVS could be affected by the shipping process and that these animals might differ from a cohort bred in-house. Another experimental consideration is that CVS and no-CVS rats received different amounts of handling due to the twice-daily presentation of stressors. Although this could be a potential confound, previous studies from our group found no differences between twice-daily–handled controls and unhandled controls (55).

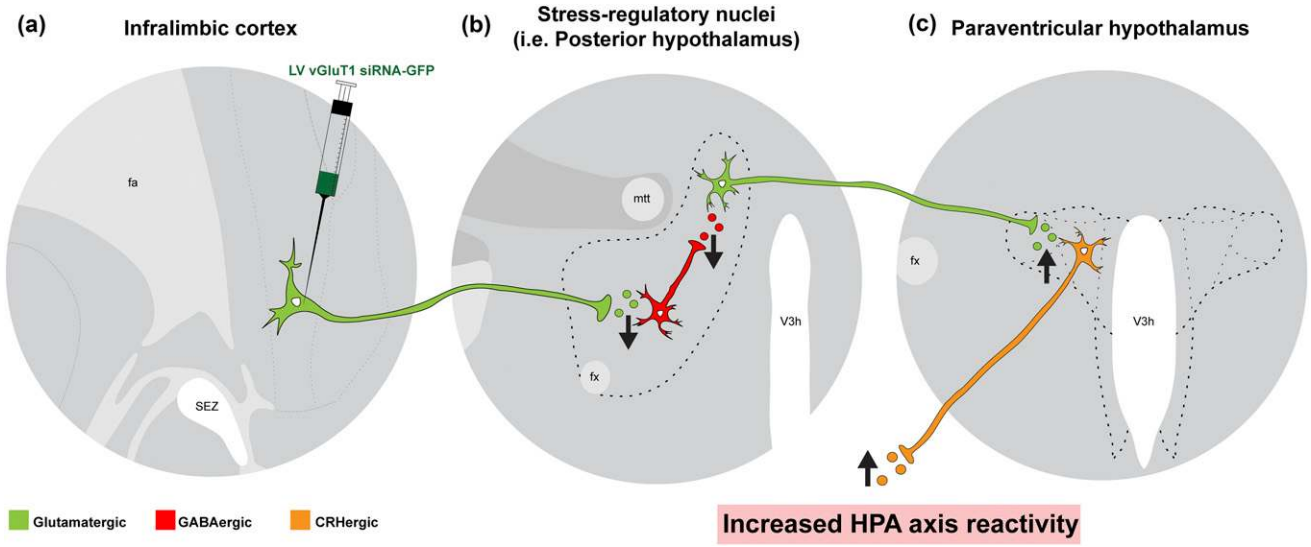

Figure 8. Hypothesized circuitry mediating IL effects on HPA axis. (a) The current study used a lentiviral-packaged vector coding for a vGluT1 siRNA conjugated to GFP that was injected into the IL. Reduced expression of vGluT1 decreases glutamate packaging and release. (b) As the removal of excitatory output facilitated HPA axis activity, we hypothesize that the IL targets inhibitory neurons within stress excitatory regions. Although there are numerous efferent targets of the IL, we have previously demonstrated that stress-activated glutamatergic neurons of the IL target GABAergic neurons in the PH (30). The local GABAergic circuitry of the PH gates excitatory projections from the PH to PVN. (c) Consequently, decreased excitation of inhibition within the PH (or other stress regulatory nuclei) could account for enhanced excitatory drive to CRH neurons and, consequently, increased HPA axis reactivity to stress. Fa, anterior forceps of the corpus callosum; fx, fornix; mtt, mammillothalamic tract; SEZ, subependymal zone; V3h, hypothalamic third ventricle.

An additional caveat is the limitation of the GFP-vGluT1 colocalization measurement as a determinant of IL vGluT1 protein knockdown. The vGluT1 protein is localized to presynaptic terminals and, consequently, widely distributed. To facilitate protein quantification, we used GFP expression to identify IL projections and measure vGluT1 protein expression in these cells. As this measure only samples cells successfully transduced and expressing the vector, it does not represent the knockdown of vGluT1 protein in IL neurons generally.

The knockdown of vGluT1 in the IL did have substantial effects on stress-induced corticosterone secretion, which could alter corticosteroid receptor expression. As these receptors are critical for feedback control of the HPA axis, changes in their expression locally within the mPFC or at other sites of feedback, such as the pituitary, could represent a potential mechanism to further understand the role of the IL in neuroendocrine adaption to chronic stress.

Conclusion

The IL and its human homolog Brodmann area 25 are critical for appraisal, reactivity, and mood (13, 15). Our current study extends our understanding of how this region regulates endocrine stress reactivity and identifies a region- and cell type–specific mechanism for endocrine disruptions frequently associated with chronic stress and stress-related illness. Future studies aimed at deciphering the circuitry of endocrine-autonomic integration could yield novel interventional targets for numerous psychiatric and cardiometabolic conditions. Particularly, identifying mechanisms of excitatory/inhibitory balance in the IL could provide a means to normalize endocrine stress reactivity and promote resilience.

Appendix. Antibody Table

Peptide/Protein Target	Manufacturer, Catalog No.	Species Raised in; Monoclonal or Polyclonal	Dilution	RRID
GFP	Invitrogen, A-11122	Rabbit; polyclonal	1:1000	AB_221569
vGluT1	Synaptic Systems, 135 303	Rabbit; polyclonal	1:1000	AB_887875
NeuN	Millipore, MAB377	Mouse; monoclonal	1:200	AB_2298772
GFAP	Dako, Z0334	Rabbit; polyclonal	1:2000	AB_10013382
Iba-1	Abcam, ab108539	Rabbit; polyclonal	1:75	AB_10862652

Abbreviation: RRID, Research Resource Identifier.

Acknowledgments

The authors thank Karen K. Ryan, Dayna Wick-Carlson, and Brittany Smith for assistance with blood sampling; Sriparna Ghosal, Ben Packard, and Dayna Wick-Carlson for assistance in tissue collection; and Sebastian Pace for contributing to illustrations.

Financial Support: This work was supported by National Institutes of Health Grants MH049698 (to J.P.H.), MH069860 (to J.P.H.), and HL122454 (to B.M.) and American Heart Association Grant 13POST17070152 (to B.M.).

Correspondence and Reprint Requests: Brent Myers, PhD, Department of Biomedical Sciences, Colorado State University, 1617 Campus Delivery, Fort Collins, Colorado 80523. E-mail: brent.myers@colostate.edu.

Disclosure Summary: The authors have nothing to disclose.

References

1. Myers B, McKlveen JM, Herman JP. Glucocorticoid actions on synapses, circuits, and behavior: implications for the energetics of stress. *Front Neuroendocrinol*. 2014;**35**(2):180–196.
2. Picard M, Juster R-P, McEwen BS. Mitochondrial allostatic load puts the 'gluc' back in glucocorticoids. *Nat Rev Endocrinol*. 2014; **10**(5):303–310.
3. de Kloet ER, Joëls M, Holsboer F. Stress and the brain: from adaptation to disease. *Nat Rev Neurosci*. 2005;**6**(6):463–475.
4. Herman JP, Figueiredo H, Mueller NK, Ulrich-Lai Y, Ostrander MM, Choi DC, Cullinan WE. Central mechanisms of stress integration: hierarchical circuitry controlling hypothalamo-pituitary-adrenocortical responsiveness. *Front Neuroendocrinol*. 2003; **24**(3):151–180.
5. Herman JP, McKlveen JM, Ghosal S, Kopp B, Wulsin A, Makinson R, Scheimann J, Myers B. Regulation of the hypothalamic-pituitary-adrenocortical stress response. *Compr Physiol*. 2016; **6**(2):603–621.
6. Myers B, McKlveen JM, Herman JP. Neural regulation of the stress response: the many faces of feedback. *Cell Mol Neurobiol*. 2012; **32**(5):683–694.
7. Ulrich-Lai YM, Herman JP. Neural regulation of endocrine and autonomic stress responses. *Nat Rev Neurosci*. 2009;**10**(6): 397–409.
8. Joëls M, Baram TZ. The neuro-symphony of stress. *Nat Rev Neurosci*. 2009;**10**(6):459–466.
9. McKlveen JM, Myers B, Herman JP. The medial prefrontal cortex: coordinator of autonomic, neuroendocrine and behavioural responses to stress. *J Neuroendocrinol*. 2015;**27**(6):446–456.
10. Maier SF, Watkins LR. Role of the medial prefrontal cortex in coping and resilience. *Brain Res*. 2010;**1355**:52–60.
11. Warden MR, Selimbeyoglu A, Mirzabekov JJ, Lo M, Thompson KR, Kim S-Y, Adhikari A, Tye KM, Frank LM, Deisseroth K. A prefrontal cortex-brainstem neuronal projection that controls response to behavioural challenge. *Nature*. 2012;**492**(7429): 428–432.
12. McKlveen JM, Myers B, Flak JN, Bundzikova J, Solomon MB, Seroogy KB, Herman JP. Role of prefrontal cortex glucocorticoid receptors in stress and emotion. *Biol Psychiatry*. 2013;**74**(9): 672–679.
13. Hamani C, Diwan M, Macedo CE, Brandão ML, Shumake J, Gonzalez-Lima F, Raymond R, Lozano AM, Fletcher PJ, Nobrega JN. Antidepressant-like effects of medial prefrontal cortex deep brain stimulation in rats. *Biol Psychiatry*. 2010;**67**(2):117–124.
14. Myers-Schulz B, Koenigs M. Functional anatomy of ventromedial prefrontal cortex: implications for mood and anxiety disorders. *Mol Psychiatry*. 2012;**17**(2):132–141.
15. Mayberg HS, Lozano AM, Voon V, McNeely HE, Seminowicz D, Hamani C, Schwalb JM, Kennedy SH. Deep brain stimulation for treatment-resistant depression. *Neuron*. 2005;**45**(5):651–660.
16. Diorio D, Viau V, Meaney MJ. The role of the medial prefrontal cortex (cingulate gyrus) in the regulation of hypothalamic-pituitary-adrenal responses to stress. *J Neurosci*. 1993;**13**(9): 3839–3847.
17. Radley JJ, Arias CM, Sawchenko PE. Regional differentiation of the medial prefrontal cortex in regulating adaptive responses to acute emotional stress. *J Neurosci*. 2006;**26**(50):12967–12976.
18. Radley JJ, Gosselink KL, Sawchenko PE. A discrete GABAergic relay mediates medial prefrontal cortical inhibition of the neuroendocrine stress response. *J Neurosci*. 2009;**29**(22):7330–7340.
19. Jones KR, Myers B, Herman JP. Stimulation of the prelimbic cortex differentially modulates neuroendocrine responses to psychogenic and systemic stressors. *Physiol Behav*. 2011;**104**(2):266–271.
20. Figueiredo HF, Bruestle A, Bodie B, Dolgas CM, Herman JP. The medial prefrontal cortex differentially regulates stress-induced c-fos expression in the forebrain depending on type of stressor. *Eur J Neurosci*. 2003;**18**(8):2357–2364.
21. McKlveen JM, Morano RL, Fitzgerald M, Zoubovsky S, Cassella SN, Scheimann JR, Ghosal S, Mahbod P, Packard BA, Myers B, Baccei ML, Herman JP. Chronic stress increases prefrontal inhibition: a mechanism for stress-induced prefrontal dysfunction. *Biol Psychiatry*. 2016;**80**(10):754–764.
22. Fremeau RT Jr, Voglmaier S, Seal RP, Edwards RH. VGLUTs define subsets of excitatory neurons and suggest novel roles for glutamate. *Trends Neurosci*. 2004;**27**(2):98–103.
23. Schuske K, Jorgensen EM. Neuroscience. Vesicular glutamate transporter–shooting blanks. *Science*. 2004;**304**(5678):1750–1752.
24. Wojcik SM, Rhee JS, Herzog E, Sigler A, Jahn R, Takamori S, Brose N, Rosenmund C. An essential role for vesicular glutamate transporter 1 (VGLUT1) in postnatal development and control of quantal size. *Proc Natl Acad Sci USA*. 2004;**101**(18):7158–7163.
25. Ziegler DR, Cullinan WE, Herman JP. Distribution of vesicular glutamate transporter mRNA in rat hypothalamus. *J Comp Neurol*. 2002;**448**(3):217–229.
26. de Almeida LP, Zala D, Aebischer P, Déglon N. Neuroprotective effect of a CNTF-expressing lentiviral vector in the quinolinic acid rat model of Huntington's disease. *Neurobiol Dis*. 2001;**8**(3): 433–446.
27. Krause EG, de Kloet AD, Scott KA, Flak JN, Jones K, Smeltzer MD, Ulrich-Lai YM, Woods SC, Wilson SP, Reagan LP, Herman JP, Sakai RR. Blood-borne angiotensin II acts in the brain to influence behavioral and endocrine responses to psychogenic stress. *J Neurosci*. 2011;**31**(42):15009–15015.
28. Grillo CA, Piroli GG, Lawrence RC, Wrighten SA, Green AJ, Wilson SP, Sakai RR, Kelly SJ, Wilson MA, Mott DD, Reagan LP. Hippocampal insulin resistance impairs spatial learning and synaptic plasticity. *Diabetes*. 2015;**64**(11):3927–3936.
29. Grillo CA, Tamashiro KL, Piroli GG, Melhorn S, Gass JT, Newsom RJ, Reznikov LR, Smith A, Wilson SP, Sakai RR, Reagan LP. Lentivirus-mediated downregulation of hypothalamic insulin receptor expression. *Physiol Behav*. 2007;**92**(4):691–701.
30. Myers B, Carvalho-Netto E, Wick-Carlson D, Wu C, Naser S, Solomon MB, Ulrich-Lai YM, Herman JP. GABAergic signaling within a limbic-hypothalamic circuit integrates social and anxiety-like behavior with stress reactivity. *Neuropsychopharmacology*. 2016;**41**(6):1530–1539.
31. Bowers G, Cullinan WE, Herman JP. Region-specific regulation of glutamic acid decarboxylase (GAD) mRNA expression in central stress circuits. *J Neurosci*. 1998;**18**(15):5938–5947.
32. Myers B, Mark Dolgas C, Kasckow J, Cullinan WE, Herman JP, Dolgas CM, Kasckow J, Cullinan WE, Herman JP. Central stress-integrative circuits: forebrain glutamatergic and GABAergic projections to the dorsomedial hypothalamus, medial preoptic area, and bed nucleus of the stria terminalis. *Brain Struct Funct*. 2014; **219**(4):1287–1303.

33. Solomon MB, Loftspring M, de Kloet AD, Ghosal S, Jankord R, Flak JN, Wulsin AC, Krause EG, Zhang R, Rice T, McKlveen J, Myers B, Tasker JG, Herman JP. Neuroendocrine function after hypothalamic depletion of glucocorticoid receptors in male and female mice. *Endocrinology*. 2015;**156**(8):2843–2853.
34. Jankord R, Solomon MB, Albertz J, Flak JN, Zhang R, Herman JP. Stress vulnerability during adolescent development in rats. *Endocrinology*. 2011;**152**(2):629–638.
35. Choi DC, Furay AR, Evanson NK, Ostrander MM, Ulrich-Lai YM, Herman JP. Bed nucleus of the stria terminalis subregions differentially regulate hypothalamic-pituitary-adrenal axis activity: implications for the integration of limbic inputs. *J Neurosci*. 2007;**27**(8):2025–2034.
36. Christiansen AM, Herman JP, Ulrich-Lai YM. Regulatory interactions of stress and reward on rat forebrain opioidergic and GABAergic circuitry. *Stress*. 2011;**14**(2):205–215.
37. Solomon MB, Jones K, Packard BA, Herman JP. The medial amygdala modulates body weight but not neuroendocrine responses to chronic stress. *J Neuroendocrinol*. 2010;**22**(1):13–23.
38. Vahl TP, Ulrich-Lai YM, Ostrander MM, Dolgas CM, Elfers EE, Seeley RJ, D'Alessio DA, Herman JP. Comparative analysis of ACTH and corticosterone sampling methods in rats. *Am J Physiol Endocrinol Metab*. 2005;**289**(5):E823–E828.
39. Engeland WC, Miller P, Gann DS. Dissociation between changes in plasma bioactive and immunoreactive adrenocorticotropin after hemorrhage in awake dogs. *Endocrinology*. 1989;**124**(6):2978–2985.
40. Ulrich-Lai YM, Engeland WC. Hyperinnervation during adrenal regeneration influences the rate of functional recovery. *Neuroendocrinology*. 2000;**71**(2):107–123.
41. Ulrich-Lai YM, Engeland WC. Adrenal splanchnic innervation modulates adrenal cortical responses to dehydration stress in rats. *Neuroendocrinology*. 2002;**76**(2):79–92.
42. Swanson LW. *Brain Maps: Structure of the Rat Brain*. 3rd ed. New York, NY: Academic Press; 2003.
43. Sullivan RM, Gratton A. Lateralized effects of medial prefrontal cortex lesions on neuroendocrine and autonomic stress responses in rats. *J Neurosci*. 1999;**19**(7):2834–2840.
44. Ulrich-Lai YM, Jones KR, Ziegler DR, Cullinan WE, Herman JP. Forebrain origins of glutamatergic innervation to the rat paraventricular nucleus of the hypothalamus: differential inputs to the anterior versus posterior subregions. *J Comp Neurol*. 2011;**519**(7):1301–1319.
45. Vertes RP. Differential projections of the infralimbic and prelimbic cortex in the rat. *Synapse*. 2004;**51**(1):32–58.
46. Rubin RT, Miller TH, Rhodes ME, Czambel RK. Adrenal cortical responses to low- and high-dose ACTH(1-24) administration in major depressives vs. matched controls. *Psychiatry Res*. 2006;**143**(1):43–50.
47. Roth-Isigkeit AK, Schmucker P. Postoperative dissociation of blood levels of cortisol and adrenocorticotropin after coronary artery bypass grafting surgery. *Steroids*. 1997;**62**(11):695–699.
48. Sonntag WE, Goliszek AG, Brodish A, Eldridge JC. Diminished diurnal secretion of adrenocorticotropin (ACTH), but not corticosterone, in old male rats: possible relation to increased adrenal sensitivity to ACTH in vivo. *Endocrinology*. 1987;**120**(6):2308–2315.
49. Bornstein SR, Engeland WC, Ehrhart-Bornstein M, Herman JP. Dissociation of ACTH and glucocorticoids. *Trends Endocrinol Metab*. 2008;**19**(5):175–180.
50. Spiga F, Lightman SL. Dynamics of adrenal glucocorticoid steroidogenesis in health and disease. *Mol Cell Endocrinol*. 2015;**408**:227–234.
51. Dallman MF. Control of adrenocortical growth in vivo. *Endocr Res*. 1984-1985;**10**(3-4):213–242.
52. Engeland WC, Shinsako J, Dallman MF. Corticosteroids and ACTH are not required for compensatory adrenal growth. *Am J Physiol*. 1975;**229**(5):1461–1464.
53. Engeland WC, Dallman MF. Compensatory adrenal growth is neurally mediated. *Neuroendocrinology*. 1975;**19**(4):352–362.
54. Engeland WC, Dallman MF. Neural mediation of compensatory adrenal growth. *Endocrinology*. 1976;**99**(6):1659–1662.
55. Herman JP, Watson SJ, Spencer RL. Defense of adrenocorticosteroid receptor expression in rat hippocampus: effects of stress and strain. *Endocrinology*. 1999;**140**(9):3981–3991.